ISSN No:-2456-2165 https://doi.org/10.38124/ijisrt/25oct1013

CFD-Assisted BTMS Optimization for High-Energy-Density Cylindrical Lithium-Ion Cells

Deepak Turkar[1]; Dr. Ajay Kumar Singh[2]; Dr. Parag Mishra[3]; Bhagwat Dwivedi[4]

[1]M. Tech Scholar; [2]Professor; [3]Associate Professor; [4]Assistant Professor
[1;2;3;4]Department of Mechanical Engineering Radharman Institute of Technology and Science, Bhopal, India

Publication Date: 2025/11/13

Abstract: High-energy-density cylindrical lithium-ion batteries, such as 2170 cells, demand efficient thermal management to ensure safe operation, prolonged cycle life, and optimal performance. This study presents a computational fluid dynamics (CFD)-based optimization of a liquid-cooled Battery Thermal Management System (BTMS) incorporating novel triangular-shaped coolant passages positioned between three adjacent cells. The design enhances coolant–cell interaction, improves temperature uniformity, maintains a compact module geometry, and achieves a high volumetric packing efficiency (VPE) of 82.6%. Simulations were performed in ANSYS Fluent 2025 R1 under discharge rates of 1C, 2C, and 5C, with coolant velocities ranging from 0.005 to 0.05 m/s. Results indicate that the triangular channels effectively reduce maximum cell temperature, maintain near-zero temperature difference between cells due to symmetry, and limit pressure drop to below 90 Pa, while increasing the coolant–cell contact area per cell by 43%. These findings demonstrate that the proposed BTMS offers thermally stable, energy-efficient, and manufacturable battery modules suitable for next-generation electric vehicles.

Keywords: *Liquid Cooling; Triangular Coolant Channels; Temperature Uniformity; Thermal Optimization; Electric Vehicles; Volumetric Packing Efficiency; 2170 Cells.*

How to Cite: Deepak Turkar; Dr. Ajay Kumar Singh; Dr. Parag Mishra; Bhagwat Dwivedi (2025) CFD-Assisted BTMS Optimization for High-Energy-Density Cylindrical Lithium-Ion Cells. *International Journal of Innovative Science and Research Technology*, 10(10), 2226-2240. https://doi.org/10.38124/ijisrt/25oct1013

I. INTRODUCTION

The global transition to electric vehicles (EVs) has accelerated significantly, driven by stringent climate targets, evolving government policies, and rapid technological advancements. In 2024, worldwide EV sales reached a record 17 million units, marking a 25% increase from the previous year and accounting for over 20% of all new car sales. This surge reflects rising consumer demand alongside continuous improvements in battery technology, which remains central to EV performance. China led this growth, with over 11 million EVs sold, approximately 65% of global sales. In the first quarter of 2025, global EV sales increased by 35% year-on-year, with China continuing to dominate the market. Europe also witnessed substantial growth, with sales up 25% year-over-year in the first half of 2025. Next-generation batteries, including solid-state and sodium-ion types, are emerging as safer, more durable, and economically viable alternatives to traditional lithium-ion batteries. These innovations promise longer driving ranges, reduced charging times, and enhanced sustainability, addressing key consumer concerns and further propelling EV adoption [1].

Lithium-ion (Li-ion) batteries dominate EV applications due to their high energy density, long cycle life, and relatively low self-discharge. However, their thermal sensitivity remains a critical challenge. Safe and efficient operation requires maintaining cell temperatures within 20–40 °C and limiting the maximum temperature difference between cells to below 5 °C. Exceeding these limits can lead to performance degradation, accelerated aging, or even thermal runaway. With the increasing adoption of large-format cylindrical cells such as the 2170 type—commonly used by Tesla—issues of excessive heat generation and non-uniform temperature distribution have become critical [2,3].

Battery thermal management systems (BTMS) are essential to address these challenges. Strategies include air cooling, liquid cooling, phase change materials (PCM), and hybrid approaches [3–5]. Among these, liquid cooling has emerged as the most effective for high-energy-density modules due to its superior heat transfer capability and ability to maintain uniform temperatures [5]. The thermal and hydraulic performance of liquid-cooled BTMS strongly depends on coolant passage design. Conventional geometries—straight, U-shaped, or serpentine channels—

ISSN No:-2456-2165 https://doi.org/10.38124/ijisrt/25oct1013

present trade-offs: serpentine channels improve heat transfer and reduce hotspots but increase pressure drop and pumping power, while straight channels lower pumping effort but often result in uneven temperature distribution [6]. Lithium-ion batteries can be classified into several types, with the most common thermal management strategies illustrated in Figure 1 [7].

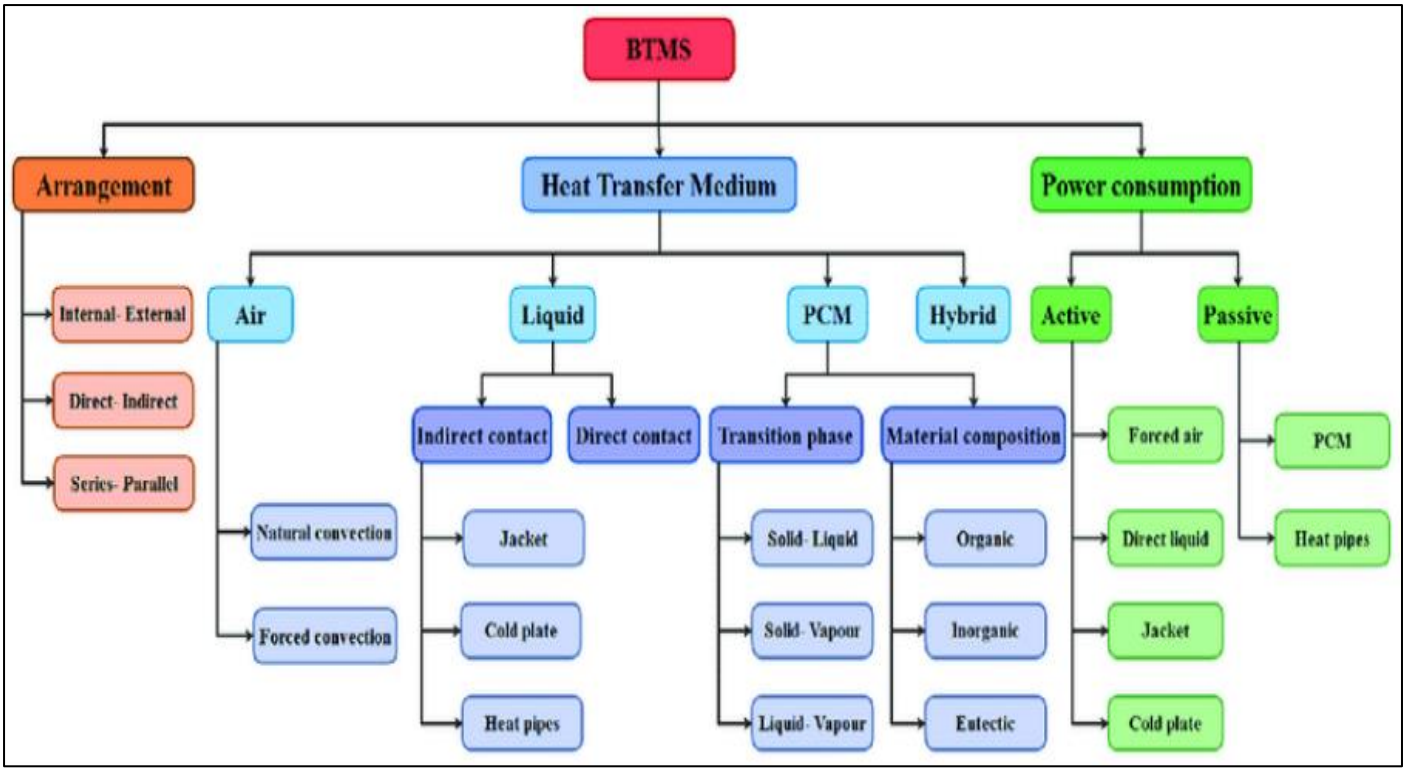

Fig 1 Classification of Thermal Management Strategies for Li-ion Batteries [7]

Recent studies have investigated innovative coolant channel geometries, including spiral, wavy, branched, and bio-inspired designs [8,9], to optimize the balance between heat transfer and hydraulic performance. While these designs enhance temperature uniformity and reduce hotspots, their practical implementation in EV battery modules remains limited due to manufacturing and integration constraints. This challenge is further exacerbated by high-power fast charging and increasingly dense cell packing, both of which substantially elevate heat generation rates [10].

➢ *Motivation:*

This study proposes triangular-shaped coolant passages positioned between three adjacent 2170 cylindrical cells. Unlike conventional straight or serpentine channels, triangular-shaped passages aim to enhance surface contact, improve coolant distribution, increase volumetric packing efficiency, simplify manufacturing, and balance heat transfer with pressure drop. Using computational fluid dynamics (CFD), the study analyzes module thermal response under varying C-rates and coolant velocities. Key performance indicators include maximum cell temperature, temperature uniformity, pressure drop, and required pumping power. This work provides design insights for next-generation BTMS, aiming to improve thermal safety, enable faster charging, and extend battery life.

II. REVIEW OF LITERATURE

Thermal management is a critical challenge in high-energy-density cylindrical lithium-ion battery packs for electric vehicles, as excessive temperatures and non-uniform heat distribution can degrade performance, reduce cycle life, and pose safety risks. Among various thermal management strategies, liquid cooling has been widely recognized as the most effective method to maintain uniform cell temperatures and prevent thermal runaway. Both experimental investigations and computational fluid dynamics (CFD) studies have contributed to understanding the performance of various cooling designs, channel geometries, and hybrid strategies.

- Hosseini Moghaddam 2021 [11] performed CFD simulations on 18650 and 21700 cylindrical modules to optimize liquid cooling channel designs. The study analyzed straight, serpentine, and compact channels under a volumetric heat generation rate of 2 W per cell. Results demonstrated that optimized serpentine and compact channels reduced maximum cell temperature by 8–10 °C and improved temperature uniformity by 2–3 °C. Vertical cell arrangements further minimized hotspots compared to horizontal layouts, and higher coolant velocity enhanced thermal performance while increasing pumping power(Fig 2).

ISSN No:-2456-2165 https://doi.org/10.38124/ijisrt/25oct1013

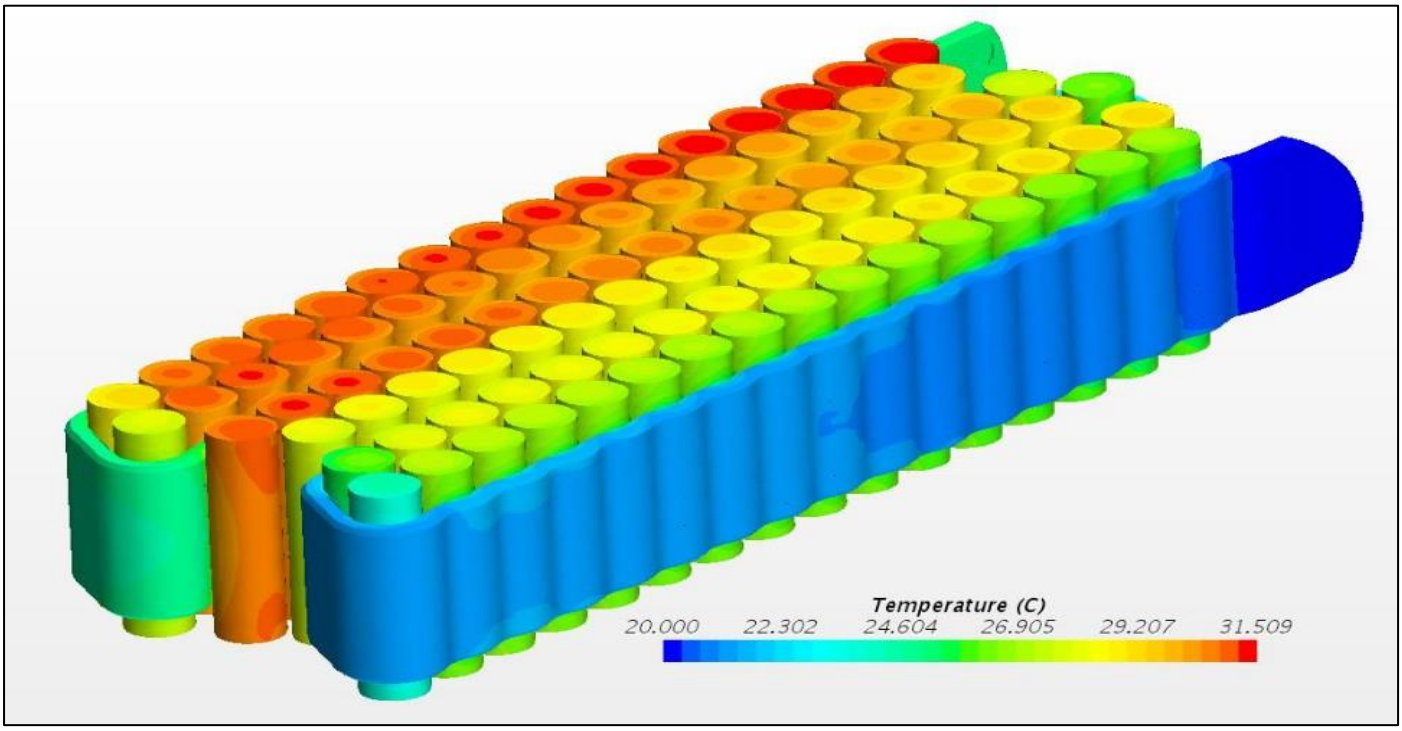

Fig 2 Temperature Distribution in a Module with Tube Cooling at 2W/Cell

- Murphy and Akrami 2022 [12] conducted a comparative CFD study of vertical, horizontal, and optimized liquid cooling arrangements. Their optimized design achieved a maximum cell temperature of 301.31 K and a temperature gradient of 1.144 K, highlighting the critical role of flow orientation in achieving uniform thermal distribution.
- Afraz et al. 2022 [13] proposed a compact liquid cooling approach for Tesla-type packs. CFD simulations revealed that carefully optimized channel design maintained temperature variation within 2 °C across the module. Afraz et al. 2021 [14] also investigated cooling plate thickness and flow rate optimization, concluding that 2 mm plates with a 0.6 L/min flow rate offered the best trade-off between cooling efficiency and pumping losses.
- Lv et al. 2022 [15] experimentally investigated a hybrid cooling method combining conventional liquid coolant with graphene-modified silica gel. This strategy reduced maximum cell surface temperature by ~6 °C relative to conventional liquid cooling, demonstrating the potential of hybrid materials for enhancing thermal management.
- Hariprasath et al. 2023 [16] explored the use of nanofluids (Al_2O_3, CuO, TiO_2, SiO_2, graphene oxide) for liquid cooling of a 52-cell cylindrical module. The study reported up to 15% improvement in heat dissipation, although the enhanced thermal performance was accompanied by increased pressure drop, highlighting a trade-off between cooling efficiency and pumping power.
- Sahu et al. 2022 [17] compared microchannel cooling using water and ethylene glycol. Water provided lower pressure drop (~741 Pa), while ethylene glycol improved cooling at the cost of higher pumping power (~1557 Pa), emphasizing the need to balance thermal performance and system efficiency.
- Wang et al. 2021 [18] performed immersion cooling experiments on a 60-cell cylindrical pack, showing that a 0.5 L/min coolant flow at 2C discharge effectively maintained maximum temperature below 45 °C. Higher flow rates enabled operation at 6.5C discharge while preventing thermal runaway, demonstrating the capability of immersion cooling for high-rate applications.
- Zhang et al. 2022 [19] introduced half-helical duct channels for cylindrical cells. CFD results indicated a 12% reduction in maximum temperature and improved uniformity compared to linear channels, suggesting the importance of channel geometry in heat dissipation.
- Lee and Kim 2023 [20] investigated non-conventional geometries, including kite-shaped and chamfered triangular ducts for 21700 cells, using CFD coupled with machine-learning optimization. Kite-shaped channels reduced maximum temperature rise by 4.2 °C and improved uniformity by 18%, illustrating the benefits of combining geometric optimization with computational intelligence.
- Jeon et al. 2022 [21] compared multi-counter, parallel, and counter-flow liquid cooling channels. The multi-counter design reduced maximum temperature by 4–5 °C and improved temperature uniformity by ~3 °C, while avoiding excessive pressure drop, confirming the effectiveness of advanced multi-counter geometries.
- Wang and Ye 2022 [22] optimized structural parameters such as the number of channels, contact angles, and inlet velocity for cylindrical power battery modules. Optimized contact angles reduced maximum temperature by 3–4 °C, and increasing the number of channels improved thermal uniformity marginally.
- Ling et al. 2023 [23] developed minichannel cold plates for cylindrical cells. Optimized channel geometry (width 1–2 mm, depth 2–3 mm) and coolant velocities of 0.1–0.5 m/s reduced peak temperatures by 4–5 °C, providing practical design rules for effective cooling plates.

ISSN No:-2456-2165 https://doi.org/10.38124/ijisrt/25oct1013

- *Summary of Literature*

Across these studies, several critical insights emerge:

✓ Channel Geometry and Flow Orientation: Serpentine, half-helical, multi-counter, and kite-shaped designs consistently outperform simple straight channels in reducing peak temperatures and improving uniformity. Vertical flow orientation helps minimize hotspots.
✓ Coolant Selection and Hybridization: Water and ethylene glycol are standard coolants, but hybrid approaches (e.g., graphene-enhanced materials, nanofluids) can further improve heat dissipation at the cost of increased pumping power.
✓ Plate and Channel Design Optimization: Cooling plate thickness, channel dimensions, and contact angles significantly influence thermal performance. Minichannel designs provide effective solutions for compact modules.
✓ CFD and Experimental Validation: Combined CFD and experimental approaches are essential for validating designs and ensuring reliability under high C-rate conditions.

These studies collectively demonstrate that advanced CFD-based optimization, coupled with innovative channel geometries and hybrid cooling materials, is essential for the next generation of effective and scalable battery thermal management systems for high-power cylindrical Li-ion cells.

- *Research Gap*

Despite extensive studies on cylindrical Li-ion battery thermal management, several gaps remain:

✓ Limited Exploration of Advanced Geometries: Most studies focus on conventional straight, serpentine, or simple non-conventional channels, while triangular-shaped coolant passages for 21700 cells remain underexplored.
✓ Insufficient Pack-Level Evaluation: Few investigations systematically assess nanofluids or hybrid cooling strategies at the full-module level, especially considering the trade-off between thermal performance and pumping power.
✓ Minimal Use of AI-Based Optimization: AI-driven surrogate modeling, which can accelerate design iterations and optimize multi-parameter BTMS performance, has seen limited adoption in the field.
✓ Techno-Economic and Scalability Considerations: Practical implementation challenges—including cost, energy consumption, and scalability under realistic charge/discharge cycles—are largely underexplored.

III. METHODOLOGY

This study employs computational fluid dynamics (CFD) simulations to evaluate the thermal performance of a Tesla Model 3 2170-cell lithium-ion battery module using triangular-shaped liquid cooling passages. The methodology aims to analyze key thermal performance indicators, including temperature distribution, maximum cell temperature, cell-to-cell temperature uniformity, and pressure drop under varying discharge rates (C-rates) and coolant velocities. The CFD approach allows for precise investigation of heat transfer phenomena without requiring extensive experimental testing, while also enabling parametric studies for optimization of coolant channel design, flow rates, and module geometry.

➢ *Battery and Geometry Model*

The battery module consists of 2170 cylindrical lithium-ion cells, each with a diameter of 21 mm and a height of 70 mm. The cells are arranged in a hexagonal close-packed configuration, maximizing packing efficiency while maintaining space for triangular coolant channels between adjacent cells. This arrangement enhances the cell-to-coolant contact area, ensuring efficient heat removal and improved temperature uniformity across the module. Figure 3 showing the position of the cooling tube inserted between cells with inlet and outlet.

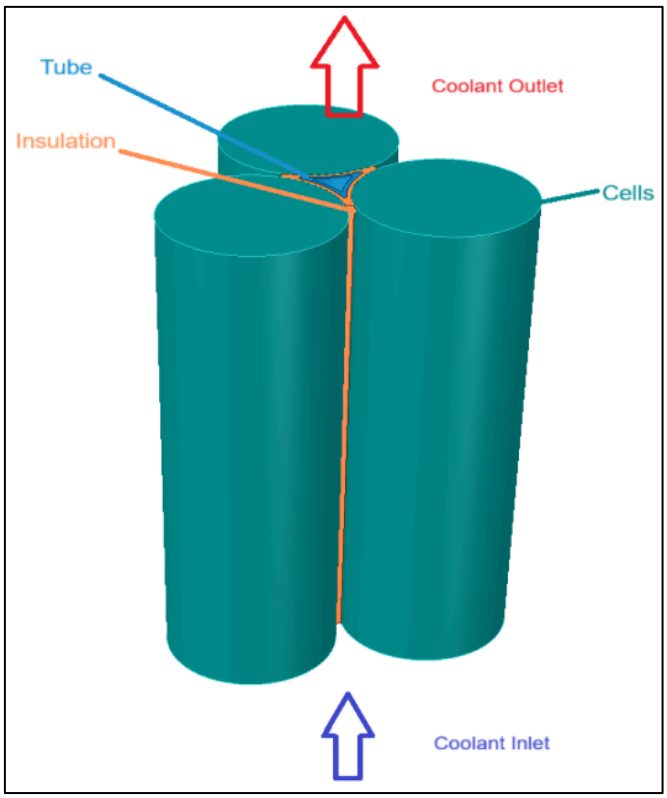

Fig 3 Single Tube with Inlet and Outlet).

Each cell is modeled as a solid cylindrical domain, with a uniform volumetric heat generation term representing the internal electrochemical losses during charge and discharge cycles. The cells are in direct thermal contact with an aluminum support structure (Al 6061-T6), which acts both as a structural framework and a thermal conduction path. This support ensures uniform heat spreading and maintains mechanical stability of the battery module.

To electrically isolate cells from the aluminum contact structure while allowing thermal conduction, a 0.5 mm thick silicon-based thermal pad is applied between each cell and the aluminum wall. This pad provides adequate insulation to prevent electrical shorting and ensures effective heat transfer from the cell to the coolant channels.

ISSN No:-2456-2165 https://doi.org/10.38124/ijisrt/25oct1013

The coolant, a 50:50 mixture of water and ethylene glycol, flows through the triangular channels positioned between three adjacent cells. The triangular shape is designed to maximize the contact area between the coolant and cell surfaces, increasing heat transfer efficiency without significantly increasing module volume. Inlet velocity and temperature are specified according to operational requirements 0.05, 0.01, 0.005m/s and 298K, and the outlet is maintained at atmospheric pressure.

To reduce computational expense while maintaining accurate results, one-sixth of the 3 cells are modeled with symmetry boundary conditions because all tubes will have the same working conditions and each tube is touching 3 cells, capturing realistic coolant interaction and ensuring accurate representation of conjugate heat transfer phenomena. The computational domain consists of both solid regions (cells, aluminum tubes, insulation) and fluid regions (coolant channels).

The volumetric packing efficiency of the designed module—defined as the ratio of total cell volume to the total module volume. This configuration provides maximum packing efficiency possible for liquid cooling.

The contact area of the cell with cooling tubes is also maximum with the cell surface calculated in percentage of the cell surface that is in contact with the cooling tubes. Calculated as the contact area of the cell is in contact with the cooling tubes divided by the total area of the Li-ion cell.

The geometry was created in ANSYS SpaceClaim and meshed in ANSYS Fluent Meshing, generating a hybrid mesh with refinement near solid-fluid interfaces to capture boundary layer effects. Ensuring grid independence and accurate prediction of thermal and hydraulic behavior.

➢ *Heat Generation Modeling*

Internal heat generation in each cell is modeled as a uniform volumetric source term, with values based on C-rate dependent discharge conditions. Literature-reported values [25] are adopted as follows:

- 1C: 37,121 W/m³ (normal operation)
- 2C: 115,487 W/m³ (high load, fast charging/discharging)
- 5C: 188,716 W/m³ (extreme thermal scenario, potential thermal runaway) The governing expression for volumetric heat generation is:

$$q = \frac{I \cdot (V_{oc} - V)}{U_{cell}} \quad \text{(Eq.1)}$$

Where:

- I = discharge current (A) = C-rate × Capacity (Ah)
- V_{oc} = open circuit voltage (V)
- V = operating voltage (V)
- U_{cell} = cell volume (m³)

This approach allows for realistic simulation of thermal loads without requiring experimental setups. However, actual heat generation may vary with operating conditions, internal resistance, and ambient temperature, so the simulation provides a generalized yet accurate approximation for thermal assessment.

➢ *Coolant Channel Design*

Triangular liquid channels are placed between three adjacent cells, offering high contact area and compact packing. Figure 4 showing top view of the single tube with 3 cells touching its surface.

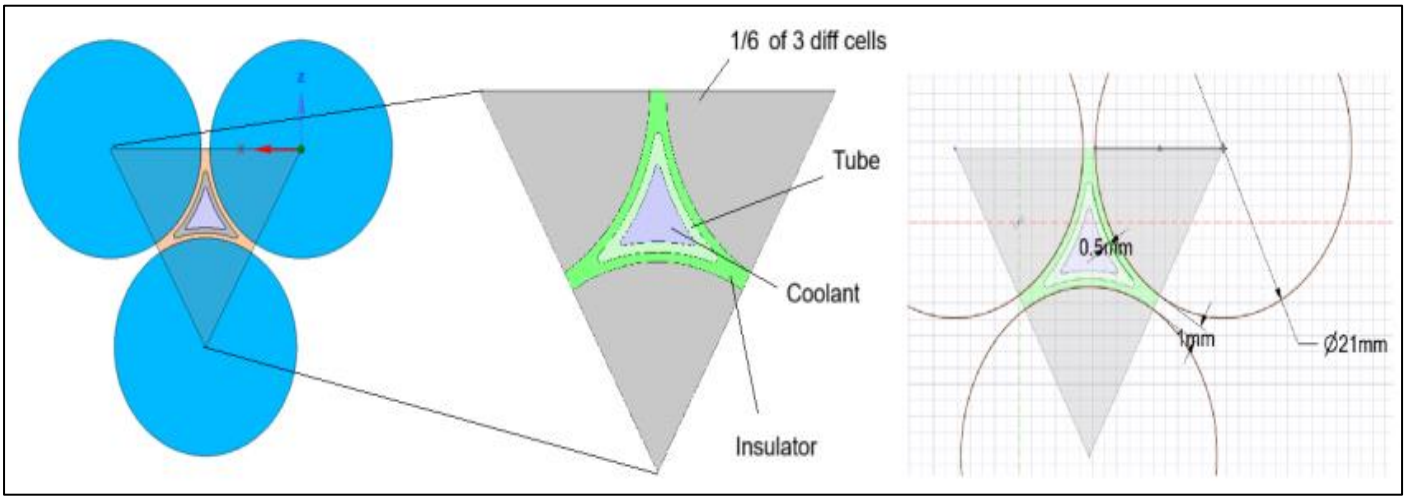

Fig 4 Top View of the Triangular Tube Passage with 3 Adjacent 1/6 Cells. The Coolant is a 50/50 Ethylene Glycol–Water Mixture with the Following Properties:

Table 1 Coolant Properties used for Simulations.

Coolant	Ethylene glycol 50/50
ρ	1074.7 kg/m³
Cp	3419.4 J/kg K

ISSN No:-2456-2165 https://doi.org/10.38124/ijisrt/25oct1013

k	0.36755 W/mk
μ	0.00402 kg/m.s

Inlet velocity is varied from 0.005 to 0.05 m/s at 298 K, with pressure outlet set to 0 Pa gauge.

➢ *Numerical Setup*

- The geometry is discretized using a hybrid mesh, with refinement at solid–fluid interfaces.
- A grid-independence study ensures numerical accuracy.
- Simulations are performed in ANSYS Fluent 2025 R1 using a steady, pressure-based solver.
- The laminar model is used to capture boundary layer effects.
- Pressure–velocity coupling is handled using the SIMPLE scheme, while momentum and energy equations are solved with second-order discretization.
- Calculation for Reynolds number

$$\mathrm{Re} = \frac{\rho v D_h}{\mu} \quad \text{(Eq. 2)}$$

Where:

- ρ= coolant density (kg/m³)
- v = inlet velocity (m/s)
- μ = dynamic viscosity (Pa·s)
- D_h = hydraulic diameter of the triangular channel (m)

The hydraulic diameter for a non-circular channel is:

$$D_h = \frac{4 \times Flow\ Area}{Perimeter} = \frac{4 \times A}{P} \quad \text{(Eq.3)}$$

From the design, we have

Perimeter of the inlet = 14.0821mm Area of inlet = 8.4606 mm²

$$D_h = \frac{4 \times 8.4606}{14.0821} \approx 2.402 \times 10^{-3}\ \mathrm{m}$$

= 2.402 mm

Now, for **Re**, inlet velocities (u = 0.005, 0.01, 0.05 m/s)

$$\mathrm{Re} = \frac{1074.7 \times v \times 2.402}{0.00402} \quad \text{(From Eq.1)}$$

- (u = 0.005) m/s → (Re ≈ 3.21)
- (u = 0.01) m/s → (Re ≈ 6.42)
- (u = 0.05) m/s → (Re ≈ 32.1)

All values are well below 2300, confirming laminar flow in triangular channels.

➢ *Boundary Conditions:*

- Heat source: volumetric generation (1C–5C)
- Tube: aluminum properties (Al 6061-T6)
- Insulation: low electric conductivity silicon pad

➢ *Convergence Criteria*

Simulation convergence is defined as:

- Residuals below 10^{-3}or continuity and momentum
- Residuals below 10^{-6} for energy

Convergence is further verified by monitoring the maximum cell temperature and coolant outlet temperature until stable. This ensures that simulation results are physically realistic and reliable.

➢ *Key Performance Indicators*

The following metrics are analyzed to evaluate BTMS performance:

- *Maximum Cell Temperature (Tmax):*

Determines the highest temperature within the module to ensure safe operation.

- *Temperature Uniformity (ΔT):*

Difference between the maximum and minimum cell's core temperatures, indicating thermal balance across the cell.

- *Pressure Drop (ΔP):*

Measures hydraulic resistance, affecting pumping power and system efficiency.

- *Effect of Coolant Velocity:*

Assesses how varying flow rates impact thermal performance and pumping requirements, helping to identify optimal coolant flow conditions.

- *Contact Area Analysis:*

Evaluates the improvement in cell–coolant interaction due to triangular channel design, compared with conventional geometries].

This methodology provides a comprehensive framework to simulate and optimize the thermal performance of high-density 2170 cylindrical battery modules under realistic operating conditions, forming a robust foundation for results and discussion sections.

IV. RESULTS AND DISCUSSION

This chapter presents CFD simulation results for the 2170-cell battery module with triangular liquid cooling tubes. Key performance indicators—maximum cell temperature, temperature uniformity, and pressure drop—are analyzed under different C-rates (1C, 2C, 5C) and varying coolant velocities.

ISSN No:-2456-2165 https://doi.org/10.38124/ijisrt/25oct1013

➢ *Packing Density*

In the battery module, cylindrical cells are interleaved with cooling tubes. The volumetric packing efficiency (VPE) is defined as the ratio of the total cell volume to the overall module volume, reflecting the space utilization and compactness of the cell arrangement within the module.

- *The Volumetric Packing Efficiency of Module with Serpentine Tubes:*

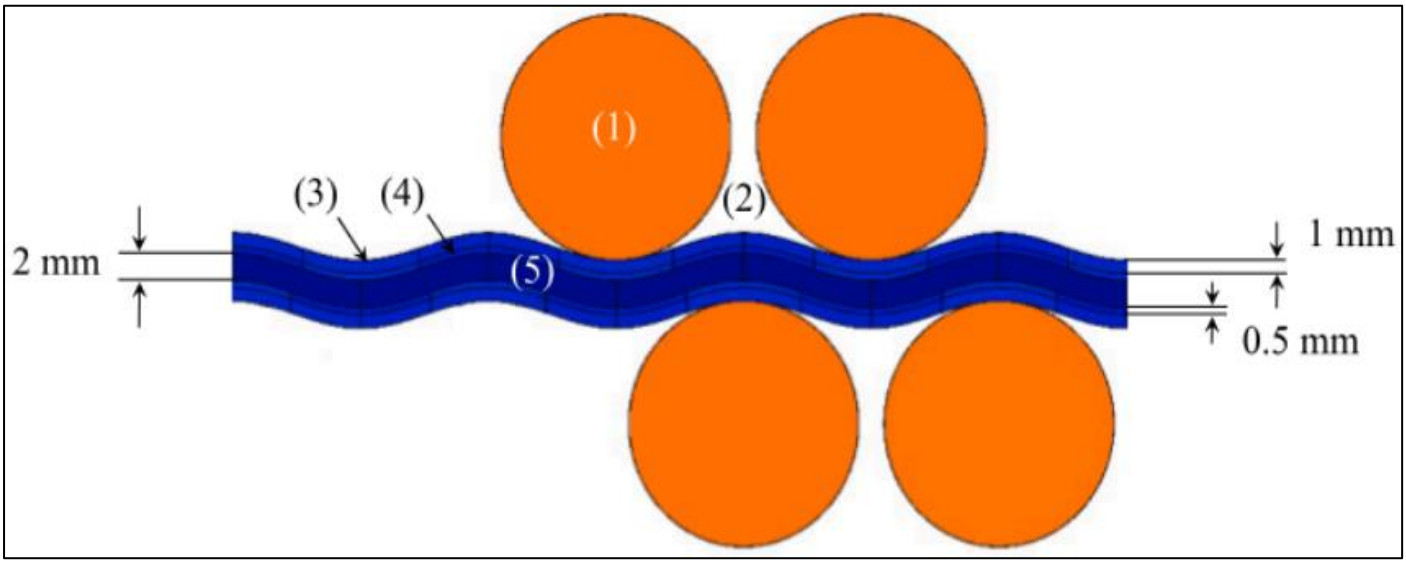

Fig 5 Details of Components and Dimensions: (1) Cell, (2) Space Between Batteries; (3) Rubber Material; (4) Cooling Channel Wall; (5) Cooling Fluid [25].

$$VPE\ (\%) = \frac{Volume\ of\ cells}{Volume\ of\ module\ portion} \times 100 \quad \text{(Eq.3)}$$

$$VPE\ (\%) = \frac{2 \times 3.14 \times 10.5^2 \times 70}{23 \times 42.5 \times 70} \times 100$$

= 70.83%

- *The Volumetric Packing Efficiency of Module with Triangular Tubes (Fig 6):*

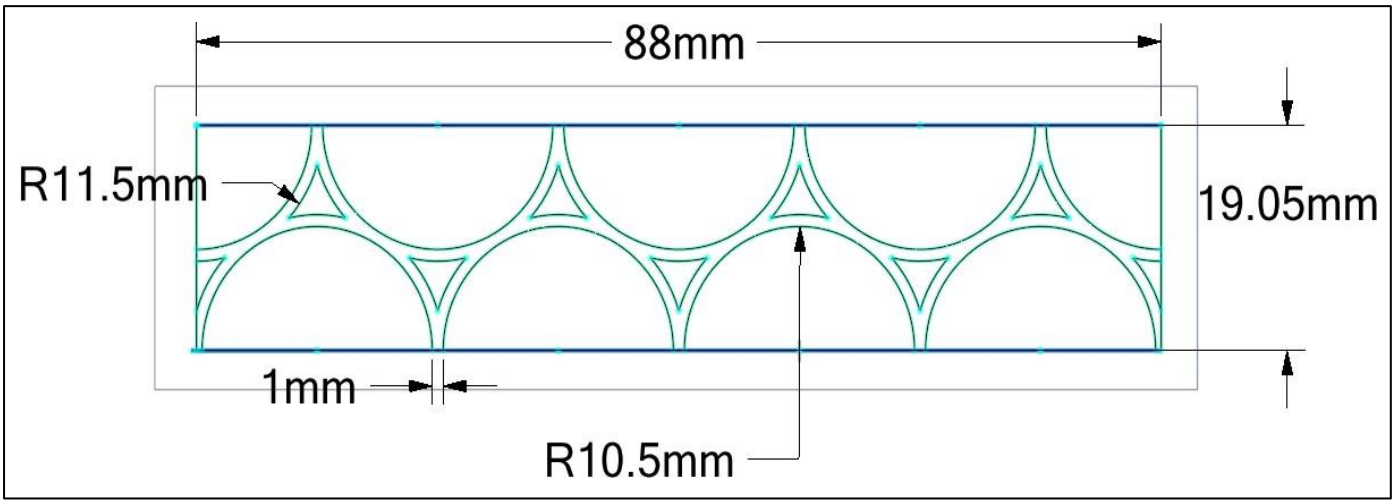

Fig 6 Top View Showing Dimensions of the Module.

Calculation for Volumetric Packing Efficiency

$$VPE\ (\%) = \frac{Volume\ of\ cells}{Volume\ of\ module\ portion} \times 100$$

$$VPE\ (\%) = \frac{4 \times 3.14 \times 10.5^2 \times 70}{88 \times 19.05 \times 70} \times 100$$

= 82.6 %

Comparison between different cylindrical cell arrangements with and without tubes (Fig 7).

ISSN No:-2456-2165 https://doi.org/10.38124/ijisrt/25oct1013

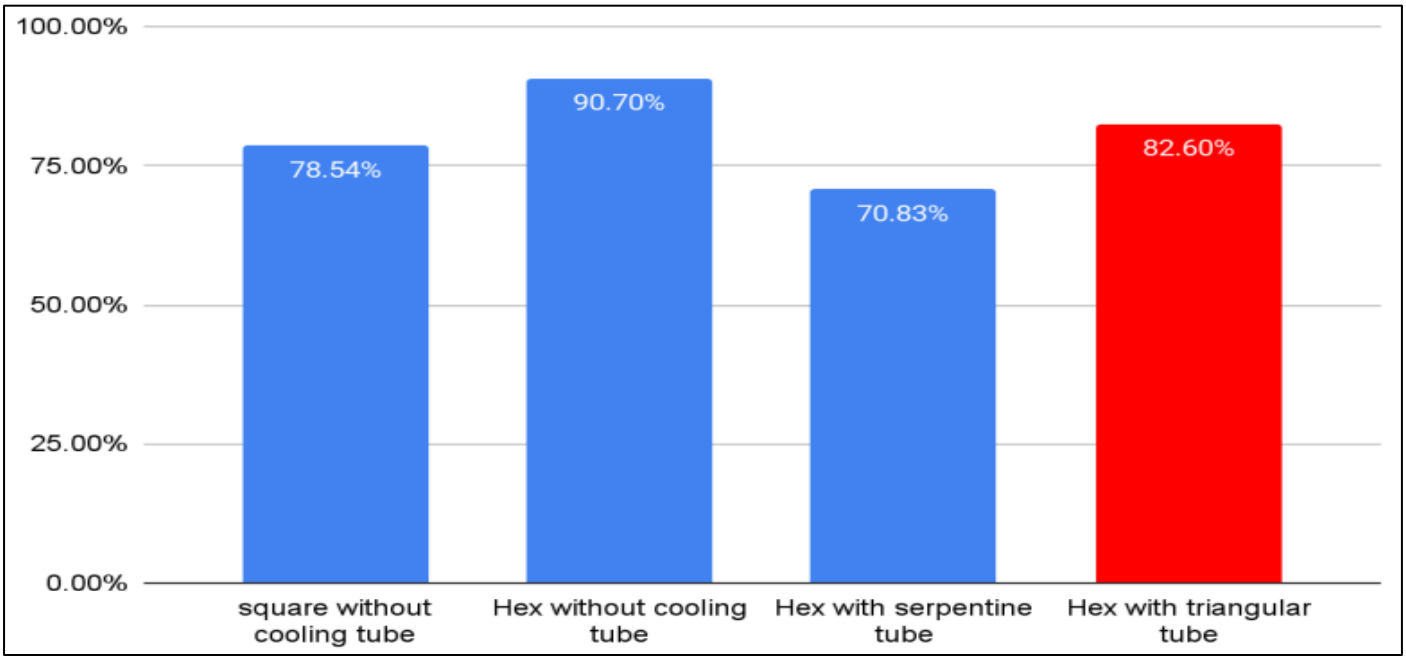

Fig 7 Comparison Between Volumetric Packing Efficiency of Different Arrangements and the Proposed Model given in Red.

The volumetric packing efficiency in the proposed model is similar to the hex arrangements without tubes but in the proposed model electric insulation is also used so the packing efficiency looks less then hex without cooling tubes, but in real scenarios it will give maximum packing efficiency among all the models.

For the proposed module design with triangular channels, the VPE is approximately 82.6%, compared to 70.83% in conventional serpentine-channel designs. This indicates a significant improvement in space utilization, enabling a more compact and energy-dense module.

➢ *Contact Area Analysis*

The performance improvement of the proposed triangular cooling configuration is strongly linked to the increase in coolant–cell contact area.

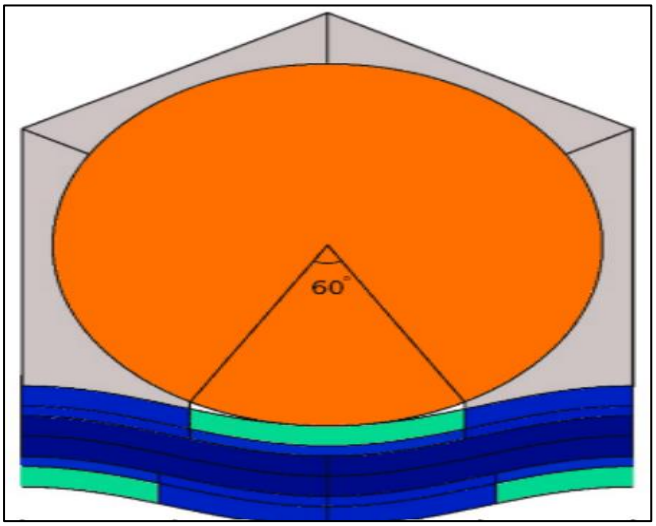

Fig 8 Contact Area in Serpentine Tube given in Green Colour [25]

$$\text{Total contact area } \% = \frac{\textit{Contact angle with the cell}}{360} \times 100$$

$$= \frac{60}{360} \times 100 = 16.67\ \%$$

In the baseline module (serpentine channel design), the effective contact interface between coolant and cells was approximately 16.67 **%** of the cell surface, as reported in previous studies.

ISSN No:-2456-2165 https://doi.org/10.38124/ijisrt/25oct1013

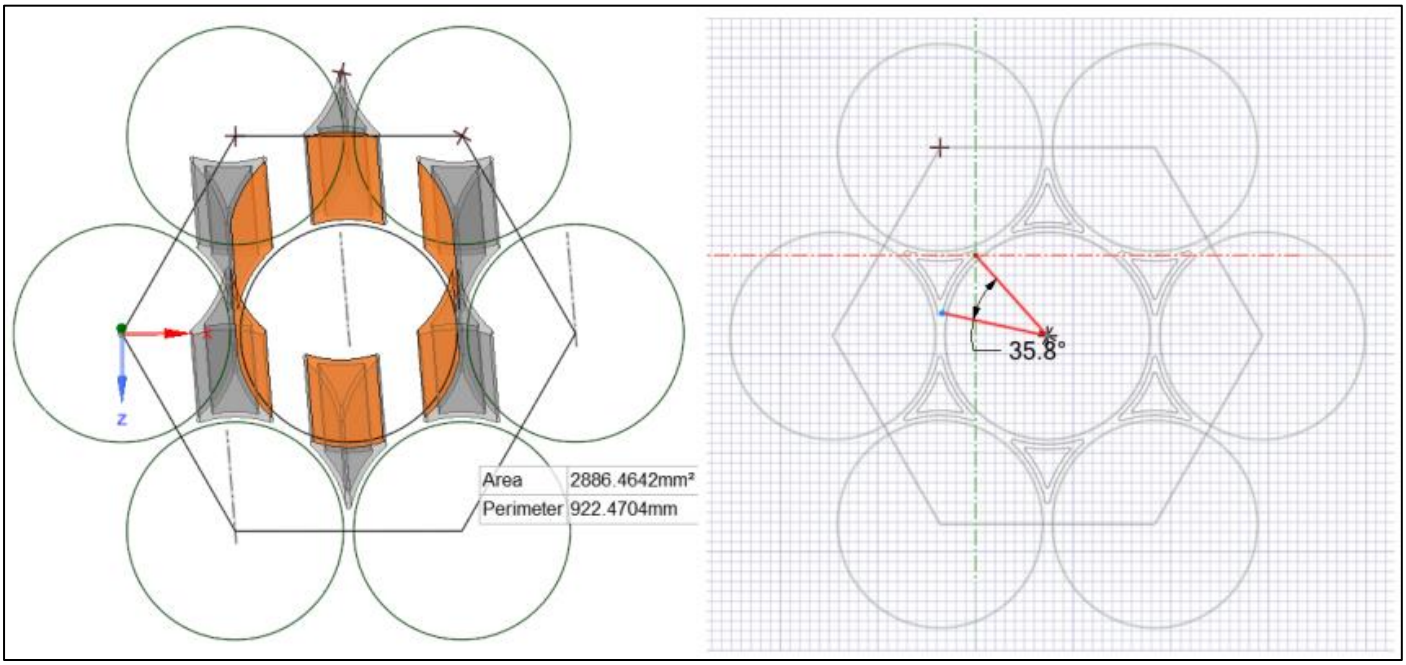

Fig 9 Contact Area in Triangular Insertions Highlighted in Orange Colour.

The total area is not directly in contact with the cells due to insulation in real models also so the 0.5mm electric insulation is taken and apparent contact area is measured. The heat transfer is similar in both cases but electric insulation will have less thermal conductivity but will represent conditions. The contact area is calculated in percentage to the side of the cells:

$$\text{Total contact area } \% = \frac{\textit{Contact angle with the cell}}{360} \times 100$$

$$= \frac{(35.8 \times 6)}{360} \times 100 = \mathbf{59.67\ \%}$$

Increase in contact area = % of area of cell in contact with the tube - % of area of cell with contact in tube = 59.67 - 16.67 % = 43% increase

The redesigned triangular cooling channel increases this interface to 59.67%, offering nearly 43% improvement in surface area for heat exchange. This geometric modification directly contributes to the observed reduction in maximum temperature and improved temperature uniformity.

➢ *Temperature Distribution*

Triangular-shaped channels efficiently guide coolant through high-heat regions, reducing hotspots and enhancing heat dissipation. The maximum temperature in the cell at Velocity 0.05m/s, 0.01m/s, and 0.005m/s.

➢ *Temperature Uniformity*

Uniform temperature is critical for cell longevity and safety. The temperature difference ΔT = Tmax − Tmin indicates thermal uniformity.

- Low ΔT values confirm that triangular-shaped channels maintain uniform thermal distribution.
- Literature reports temperature difference in cells ΔT ≈ 6 – 10 K at 2C for conventional channels ; the current design will have the same temperature for all cells, so the ΔT ≈ 0K.
- The temperature difference ΔT is given is the difference in maximum and minimum core temperature of a cell.

➢ *Cell Temperature*

Volumetric heat generation increases with C-rate.Given as q_1, q_2 and q_3. The temperature contours showing different temperatures in battery cells at different heat generation and velocities are given below. The coolant exit is shown on the top side of the temperature contour so that maximum temperature of the simulation is visible on the top side of the contour. Each table is made for only one velocity and three heat generation and the rest of the velocities are given in the other respective tables. The end of the table observation is given on the basis of temperature contour of the cell.

- *Temperature Contour at 0.05m/s Coolant Velocity with Diff Heat Generation 1C, 2C and 5C (Table 2).*

q_1 = 37,121 W/m³	q_2 = 115,487 W/m³	q_3 = 188,716 W/m³

ISSN No:-2456-2165 https://doi.org/10.38124/ijisrt/25oct1013

Table 2 Temperature Contour at 0.05 m/s at Different Heat Generation

T_{max} = 299.388 K at q_1 = 37,121 W/m³, T_{max} = 301.660 K at q_2 = 115,487 W/m³, T_{max} = 303.937 K at q_3 = 188,716 W/m³.

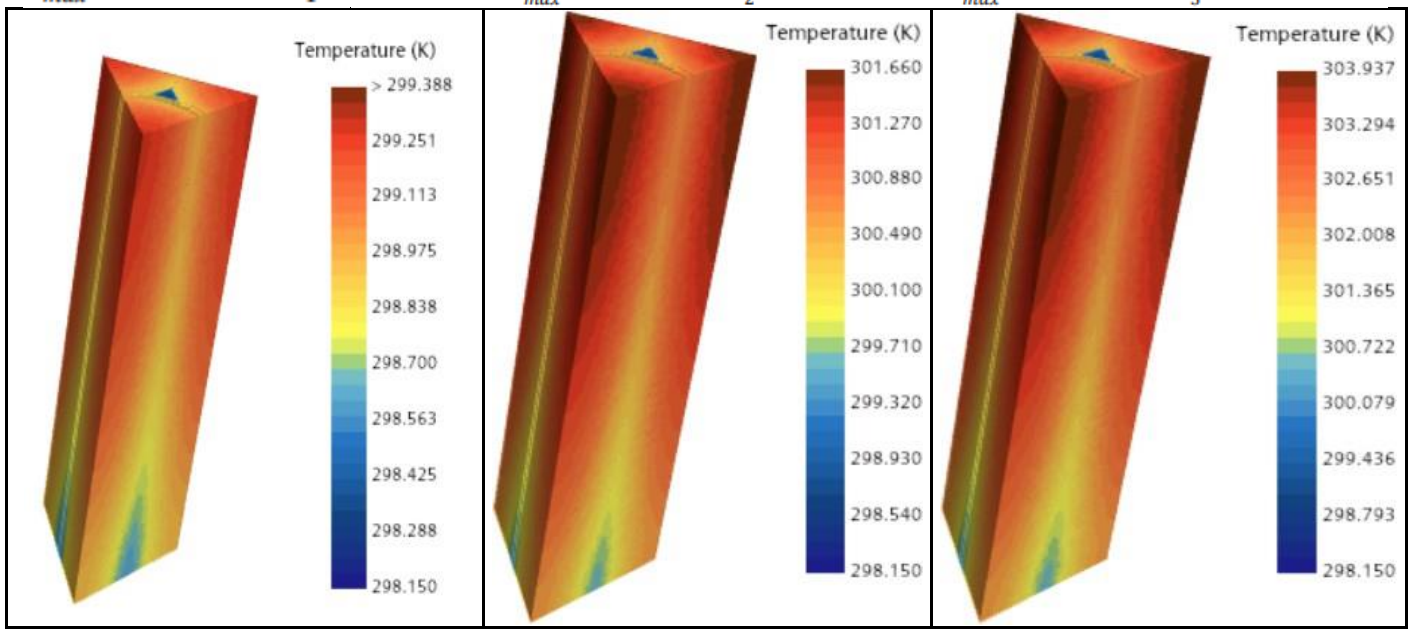

✓ *Observation:*

At coolant velocity 0.05 m/s max temperature of the cell is near 299.388 K at normal operation of lithium-ion battery (1C), 301.660 K at high load/Fast charging discharging, and 303.937 K at thermal runaway situation. So the temperature is well below safety and operation conditions. But the temperature is too low, so we can reduce pump power further.

- *Temperature Contour at 0.01m/s Coolant Velocity with Diff Heat Generation 1C, 2C and 5C (Table 3).*

q_1 = 37,121 W/m³	q_2 = 115,487 W/m³	q_3 = 188,716 W/m³

Table 3 Temperature Contour at 0.01 m/s at Different Heat Generation

T_{max} = 301.473 K at q_1 = 37,121 W/m³ , T_{max} = 306.289 K at q_2 = 115,487 W/m³, T_{max} = 310.966 K at q_3 = 188,716 W/m³.

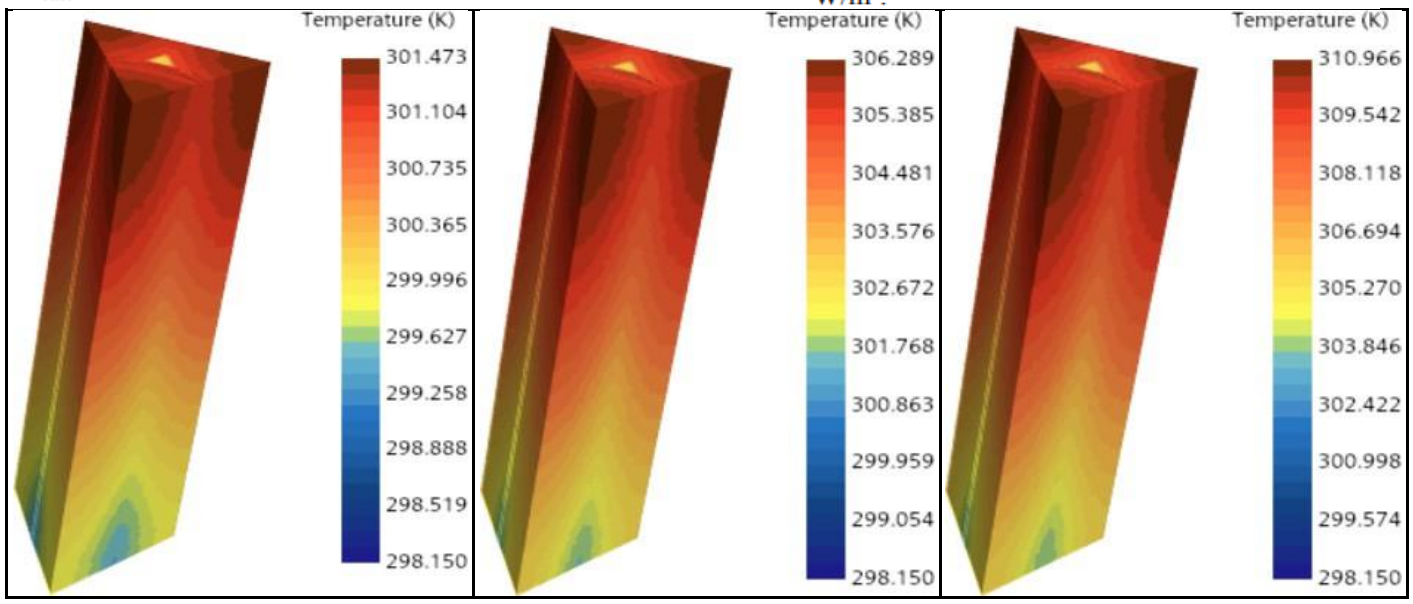

✓ *Observation:*

At coolant velocity 0.05 m/s max temperature of the cell is near 301.473 K at normal operation of lithium-ion battery (1C), 306.289 K at high load/Fast charging discharging, and 310.966 K at thermal runway situation. So the temperature is well below safe conditions, and the temperature is below the safety limit at thermal runway and operation conditions.

ISSN No:-2456-2165 https://doi.org/10.38124/ijisrt/25oct1013

➢ *Temperature Contour at 0.005m/s Coolant Velocity with Diff Heat Generation 1C, 2C and 5C (Table 4).*

q_1 = 37,121 W/m³	q_2 = 115,487 W/m³	q_3 = 188,716 W/m³

Table 4 Temperature Contour at 0.005 m/s at Different Heat Generation

T_{max} = 301.473 K at q_1 = 37,121 W/m³ , T_{max} = 306.289 K at q_2 = 115,487 W/m³, T_{max} = 310.966 K at q_3 = 188,716 W/m³.

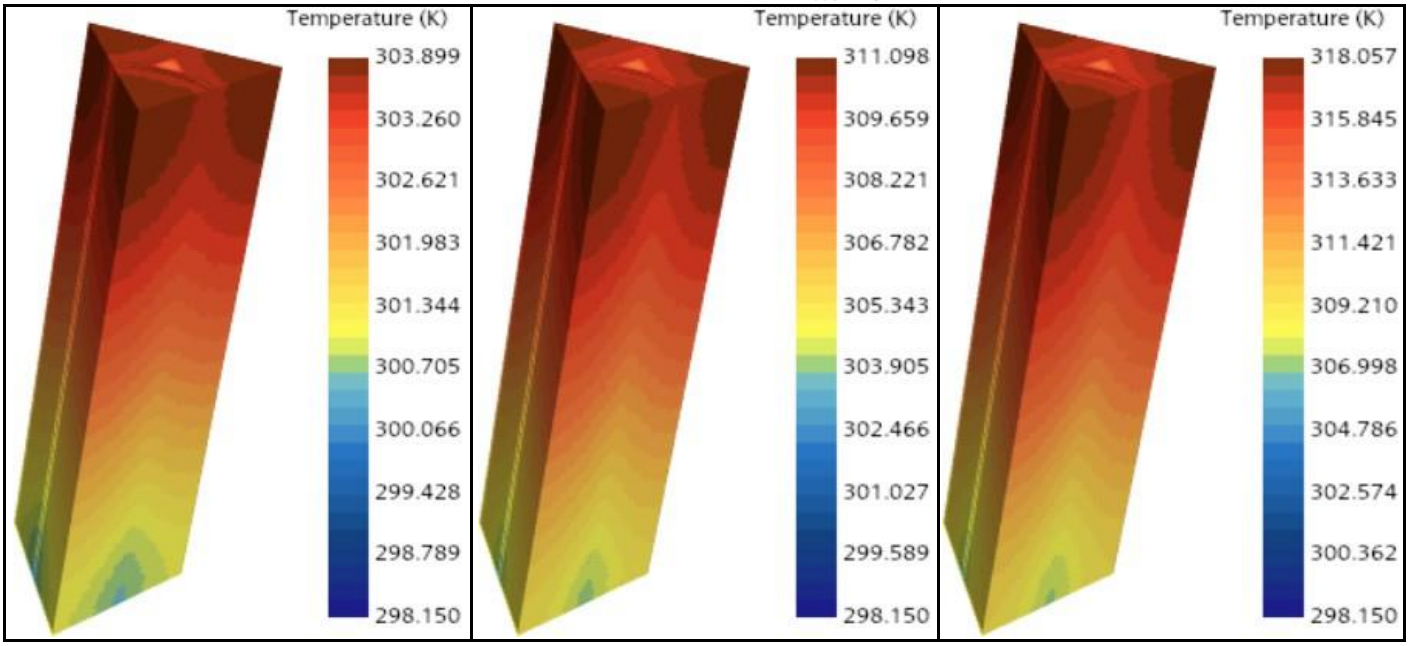

✓ *Observation:*

At coolant velocity 0.005 m/s max temperature of the cell is near 303.899 K at normal operation of lithium-ion battery (1C), 306.289 K at high load/Fast charging discharging(2C), and 310.966 K at thermal runway situation. So the temperature is well below safe conditions, and the temperature is below the safety limit at thermal runways and operation conditions(5C).

The complete table (Table 5) showing temperature and difference in core temperature in all different conditions inside the cell.

Table 5 Table Showing Maximum and Minimum and Temperature Difference inside the Core if the Battery in Difference Velocities and Heat Generations

Heat Generation (W/m³)	**Velocity (m/s)**	T_{max} **(K)**	T_{min} **(K) core**	$\Delta T_{core} = T_{max} - T_{min}$ **(K)**
37,121 (1C)	0.05	299.4	298.9	0.5
	0.01	301.5	300.5	1
	0.005	303.9	301.6	2.3
115,487 (2C)	0.05	301.7	300	1.7
	0.01	306.3	304	2.3
	0.005	311.1	306	5.1
188,716 (5C)	0.05	303.9	302.1	1.8
	0.01	311	306	5
	0.005	318	310.5	7.5

The maximum core temperature across all three airflow velocities was found to be 318 K (approximately 45 °C). Since thermal runaway is not an operational condition, this temperature remains relatively low, indicating that the system is thermally stable. Therefore, an airflow velocity of 0.005 m/s can be considered safe under all heat generation scenarios. However, if it is necessary to maintain the maximum cell core temperature below 40 °C, even under potential thermal runaway conditions, an increased airflow velocity of 0.01 m/s is recommended. Under this condition, the maximum core temperature is reduced to 311 K (approximately 38 °C), which is well within the safe operating range.

ISSN No:-2456-2165 https://doi.org/10.38124/ijisrt/25oct1013

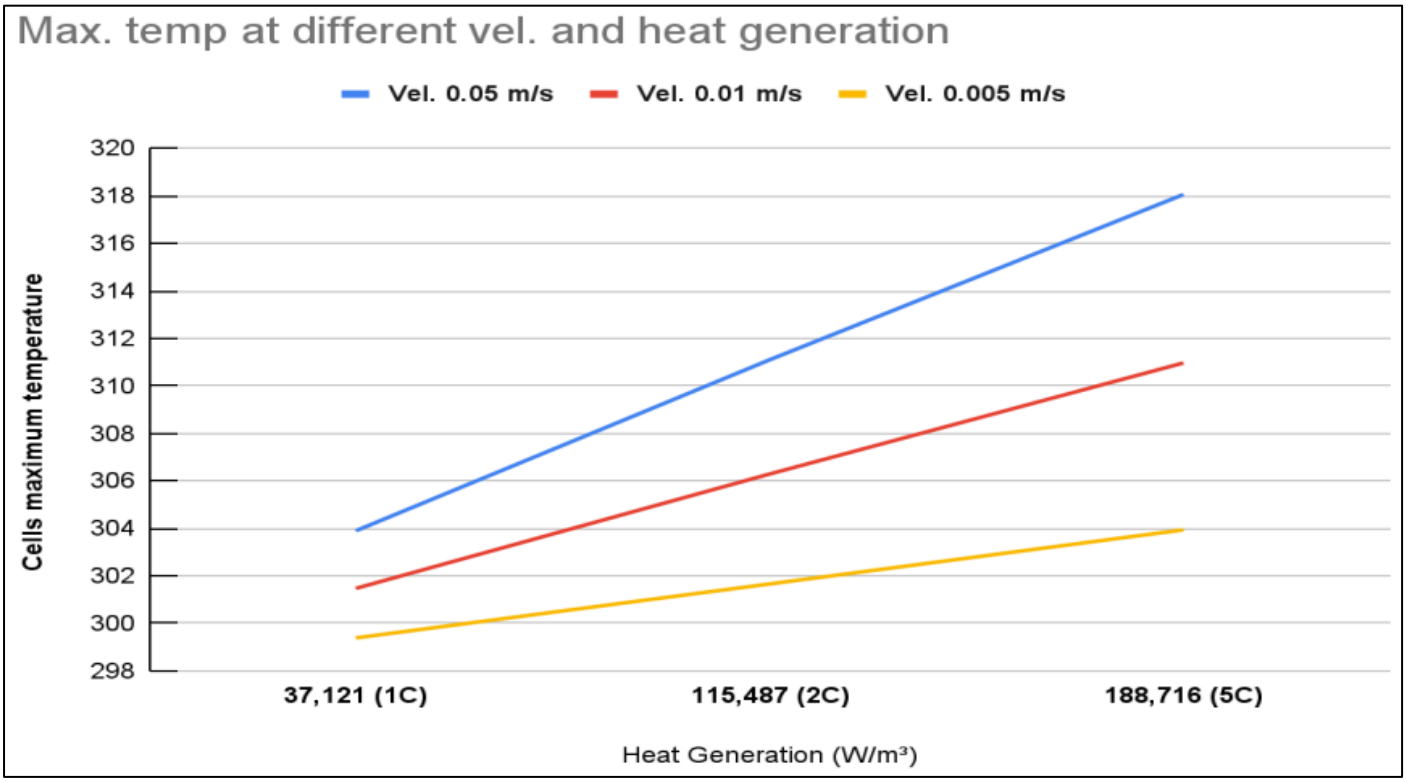

Fig 10 Relation with Maximum Temperature in the Cells and Velocity Shown in the Graph.

➢ *Pressure Drop*

Pressure drop is crucial for pumping energy and system efficiency. The pressure drops inside the tube in 3 different optimum velocities for 3 different flow rates.(Fig.10)

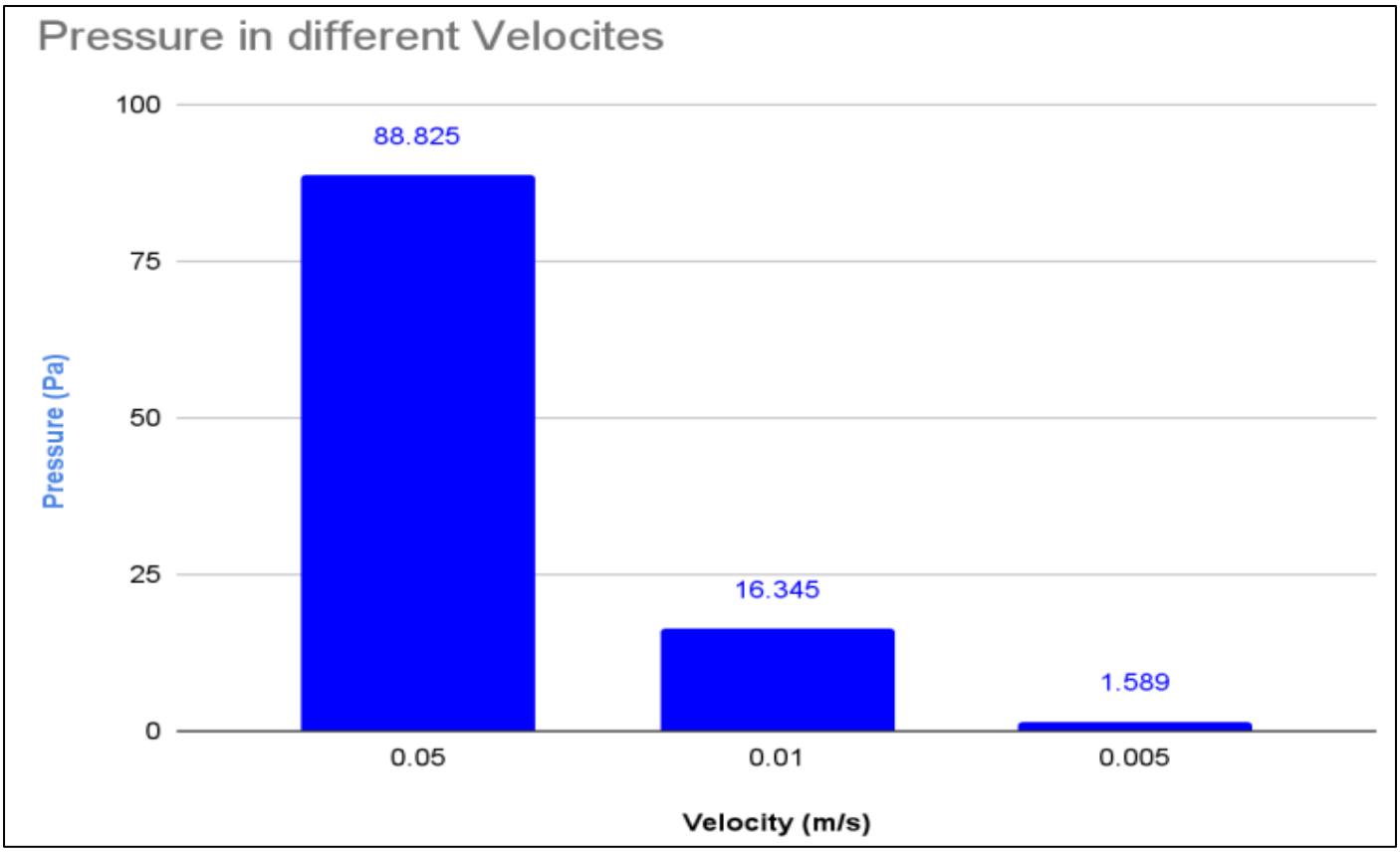

Fig 11 Graph Showing Pressure Drop Inside Tube in Different Velocities.

ISSN No:-2456-2165 https://doi.org/10.38124/ijisrt/25oct1013

➢ *Static Pressure at Velocity 0.05, 0.01, and 0.005 m/s (Fig 12)*

Static pressure in the tube at velocity 0.05m/s	Static pressure in the tube at velocity 0.01m/s	Static pressure in the tube at velocity 0.005m/s

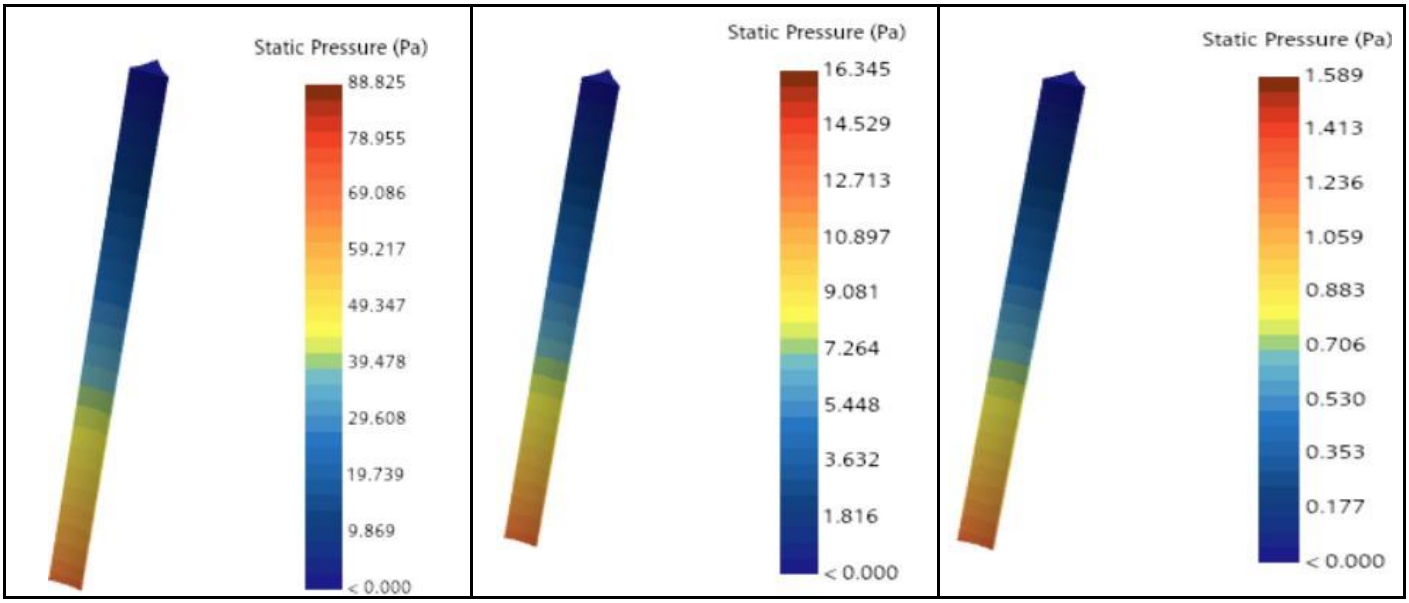

Fig 12 Static Temp at Velocity 0.05 m/s = 88.825 Pa, at 0.01 m/s = 16.345 Pa and at 0.005 m/s =1.589 Pa

- *Observation:*

Increasing coolant velocity reduces hotspots and improves temperature uniformity, though pumping power increases at higher velocities.

➢ *Effect of Coolant Flow Rate*

- Increasing coolant velocity improves heat removal and reduces ΔT.
- Excessive velocity increases pumping power.
- Optimized flow rate: 0.01 m/s balances thermal efficiency and energy consumption.

- *Observation:*

Triangular-shaped channels outperform conventional designs in maximum temperature, ΔT, and moderate pressure drop across all 6 cases.

➢ *Summary of Findings*

- Efficient heat removal and safe operating temperatures
- Low ΔT ensures uniform aging and performance
- Moderate pressure drop for energy-efficient operation
- Higher volumetric packing efficiency
- Higher tube contact area

V. CONCLUSION

CFD simulations were carried out on a Tesla 2170-cell battery module incorporating triangular liquid-cooling tubes under 1C, 2C, and 5C discharge rates at three coolant velocities.

➢ *Key Findings*

- Triangular-shaped cooling channels effectively reduce peak cell temperatures, enhance thermal uniformity, and maintain moderate pressure drops across all operating conditions.
- The increased contact area between the coolant tube and cells significantly lowers both maximum temperature and temperature variation.
- The optimized tube distribution ensures uniform flow velocity, minimizing pumping power requirements.
- The proposed design can be manufactured easily by aluminum extrusion, eliminating the need for complex machining and thereby reducing overall system cost.

➢ *Significance*

This study confirms that triangular cooling passages provide safe, energy-efficient, and thermally uniform operation for high-energy-density electric vehicle battery modules, making them a promising alternative to conventional serpentine or rectangular cooling designs.

RECOMMENDATIONS

➢ *Future Work should Focus on:*

- Transient thermal analysis under real driving and charging cycles.
- Integration of nanofluids or phase change materials (PCM) for hybrid cooling.
- Multi-module simulations to evaluate large-scale pack behavior.
- Experimental validation of CFD findings.
- Application of AI-based surrogate modeling for rapid

ISSN No:-2456-2165 https://doi.org/10.38124/ijisrt/25oct1013

thermal design optimization.

FUTURE WORK

➢ *Suggested Directions*

- Transient Analysis: Study battery temperature during charging/discharging cycles.
- Advanced Coolants: Use nanofluids or PCM to enhance heat transfer.
- Multi-Module Analysis: Evaluate scalability for larger packs.
- Experimental Validation: Prototype testing to confirm CFD results.
- Optimization & AI Modeling: Refine tube design and reduce computational effort.
- Integration with BMS: Enable active coolant flow control for improved SOC prediction.

➢ *Expected Benefits*

- Accurate prediction of thermal behavior
- Improved battery safety and longevity
- Energy-efficient, scalable cooling solutions
- Data for AI-driven thermal management

REFERENCES

[1]. International Energy Agency (IEA), Global EV Outlook 2025: Trends in Electric Car Markets, Paris, France, 2025. Available at: https://www.iea.org/reports/global-ev-outlook-2025

[2]. J. Jaguemont, L. Boulon, Y. Dubé, A comprehensive review of lithium-ion batteries used in hybrid and electric vehicles at cold temperatures, Appl. Energy 164 (2016) 99–114. https://doi.org/10.1016/j.apenergy.2015.11.034.

[3]. D. Pesaran, Battery thermal management in EVs and HEVs: Issues and solutions, Battery Man 43 (2001) 34–49.

[4]. X. Zhang, X. Wei, Y. Tang, Z. Guo, C. Song, L. Wang, A review on thermal management of lithium-ion batteries for electric vehicles, Energy 238 (2022) 121768. https://doi.org/10.1016/j.energy.2021.121768

[5]. [5]M. Saw, Y. Ye, A. Tay, Integration issues of lithium-ion battery cells into battery packs for electric vehicles – A review on mechanical, thermal and management aspects, J. Power Sources 246 (2014) 293–312. https://doi.org/10.1016/j.jpowsour.2013.07.116.

[6]. A. Bandhauer, S. Garimella, T. Fuller, A critical review of thermal issues in lithium-ion batteries, J. Electrochem. Soc. 158 (3) (2011) R1–R25. https://doi.org/10.1149/1.3515880.

[7]. Zhang X., Li Y., Wang J., Critical review towards thermal management systems of lithium-ion batteries in electric vehicles with its electronic control unit and assessment tools, Journal of Energy Storage, 34 (2021) 102091. https://doi.org/10.1016/j.est.2020.102091

[8]. Y. Rao, S. Wang, A review of power battery thermal management system technologies and development, Energy Storage Mater. 30 (2020) 301–318. https://doi.org/10.1016/j.ensm.2020.06.003.

[9]. Z. Ling, F. Wang, H. Fang, et al., A review of thermal management in lithium-ion batteries for electric vehicles: Prospects and challenges, Renew. Sust. Energy Rev. 146 (2021) 111–121. https://doi.org/10.1016/j.rser.2021.111121.

[10]. J. Jaguemont, et al., Thermal runaway mechanisms of Li-ion batteries under high C-rate charging conditions, Energy Convers. Manag. 221 (2020) 113200. https://doi.org/10.1016/j.enconman.2020.113200.

[11]. M. Hosseini Moghaddam, et al., CFD-based thermal management of Li-ion battery modules: Effect of channel design and cell arrangement, Appl. Therm. Eng. 198 (2021) 117456.

[12]. C. Murphy, B. Akrami, Comparative study on liquid cooling configurations for lithium-ion battery modules using CFD, Energy Rep. 8 (2022) 2243–2255.

[13]. S. Afraz, et al., Compact liquid cooling solutions for Tesla battery packs: A CFD study, J. Energy Storage 45 (2022) 103701.

[14]. S. Afraz, et al., Optimization of cooling plate thickness and flow rate for liquid-cooled battery packs, Appl. Energy 301 (2021) 117462.

[15]. Y. Lv, et al., Experimental study of hybrid cooling using liquid coolant and graphene-modified silica gel for cylindrical Li-ion cells, Int. J. Heat Mass Transf. 181 (2022) 121911.

[16]. K. Hariprasath, et al., Nanofluid cooling of cylindrical lithium-ion battery modules: CFD analysis of Al_2O_3, CuO, TiO_2, SiO_2 and graphene oxide, Therm. Sci. Eng. Prog. 31 (2023) 101550.

[17]. A. Sahu, et al., Comparative CFD analysis of microchannel cooling with water and ethylene glycol for battery packs, J. Therm. Anal. Calorim. 149 (2022) 4323–4336.

[18]. Q. Wang, et al., Immersion cooling of Li-ion batteries for high C-rate operation, Appl. Therm. Eng. 190 (2021) 116769.

[19]. Y. Zhang, et al., Half-helical duct cooling design for cylindrical lithium-ion battery modules, Energy Convers. Manag. 251 (2022) 114970.

[20]. S. Lee, J. Kim, CFD and machine learning-based optimization of non-conventional cooling ducts for 21700 Li-ion cells, Appl. Energy 335 (2023) 120741.

[21]. D. Jeon, et al., Performance evaluation of multi-counter liquid cooling channels for cylindrical battery modules, Int. J. Heat Mass Transf. 180 (2022) 121772.

[22]. J. Wang, Y. Ye, Optimization of liquid cooling parameters for cylindrical power battery modules using CFD, Energy 253 (2022) 123456.

[23]. Z. Ling, et al., Design and performance of minichannel cold plates for cylindrical Li-ion battery thermal management, Int. J. Heat Mass Transf. 201 (2023) 123050.

[24]. Y. Yu, et al., Thermal modeling of cylindrical

ISSN No:-2456-2165 https://doi.org/10.38124/ijisrt/25oct1013

lithium-ion cells under different C-rates: A CFD study, Electrochim. Acta 354 (2020) 136736. https://doi.org/10.1016/j.electacta.2020.136736.

[25]. Afraz, M. V., Ali Mohammadi, Z., & Karimi, G. (2024). A novel compact thermal management model for performance evaluation of Tesla-like lithium-ion battery packs. Energy Conversion and Management, 300, 117927. https://doi.org/10.1016/j.enconman.2023.117927